

Geometric accuracy assessment of remotely sensed imagery

Andre Luis da Silva Bertoncini¹
Filipe Altoé Temporim¹
Guilherme Gregório Silva¹

¹ National Institute for Space Research - INPE/SERE
Mailbox 515 - 12227-010 – São José dos Campos - SP, Brasil
{andre.bertoncini, filipe.temporim, guilherme.gregorio}@inpe.br

Abstract. Remotely sensed imagery is affected by distortions mainly caused by remote sensing platform, sensor, atmosphere, and topographic features on the surface. In order to correct these effects several methods may apply such as registration and orthorectification geometric correction. The aim of this paper is to apply a registration and orthorectification method to a high resolution image as a measure of accuracy enhancement within both techniques. To do so, images from the Geoeye-1 satellite/sensor are used, which panchromatic band has 0.5 m and multispectral bands have 2 m of spatial resolution. Ground Control Points – GCPs and a stereopair Digital Elevation Model – DEM (2 m spatial resolution) extracted for the same image are also used. Both images were classified and statistically compared to a RapidEye satellite/sensor image. The area of interest is located in the Carajás Mining Complex, in the municipality of Parauapebas, state of Pará – Brazil. Results have shown that location shifts are present between the registered and orthorectified image. There are also differences in the total area of each class, mostly on steep terrain. The statistical analysis has proved that there is improvement in the use of the orthorectification process at a 5% significance level. Thus, we could conclude that the orthorectification process is an important step on image geometric correction, contributing to enhance image metrics, morphology, and even so location accuracy.

Key-words: registration, orthorectification, supervised classification, geometric accuracy assessment.

1. Introduction

The geometry of raw high-spatial resolution images is embedded with displacement effects, derived mainly by topography, sensor, atmosphere and the remote sensing platform. These effects are caused by variations on sensor and Earth's surface geometry. The geometric correction of images is critical in studies involving the analysis of Earth's surface. Images with geometric distortions or without geometric correspondence cannot be compared to other databases, such as images of any nature, GPS data and vector data, beside they cannot be integrated into Geographic Information Systems - GIS (FREITAS et al., 2009).

In order to correct these effects, the images are registered, which is defined as the process that determines the most accurate geometrical correspondence between two or more images (FLUSSER and SUK, 1994; MAO et al., 2001). The method is based on control points, which are pairs of coordinates collected in known geographical features on the surface and in the image that is being corrected. However, according to Freitas et al. 2009, this activity requires an intensive manual labor due to the large number of control points required for a high quality geometric correction of a single image.

Several methods of geometric correction, among them the orthorectification, were developed specifically for different types of sensor's data. According to Schowengerdt (2007), the correction of terrain displacements of remotely sensed images requires a Digital Elevation Model (DEM), which consists of a spatial grid of elevation values. Geometric correction methods most used are those that use the rational polynomial coefficient – RPC which are available in the image metadata. The RPCs aim to reconstruct the sensor physical geometry in the act of collecting the image, these are rigorous methods.

The area of interest is located in the Carajás Mining Complex (Blue deposit), in the municipality of Parauapebas, state of Pará – Brazil (Figure 1). This deposit was discovered in September 1971 and the mining activities started in 1985. It is recognized internationally for the excellent quality of its ore, which contains high concentrations of Mn and high Mn-Fe

ratio. Nowadays, the Blue mining complex total area is around 2.5 km², which contains three simultaneous open pits (1, 2 and 3 mines) and a processing plant. The area comprises the Amazon rainforest, characterized by a humid forest of broadleaf trees. The region is very hilly and the highest slopes occur on the mine pits.

The aim of this paper is to compare two methods of image geometric correction (registration and orthorectification) of a high-spatial resolution image of GeoEye-1 satellite/sensor. The validation will be done by supervised classification of both images, as well as through a Root Mean Square – RMS error statistical assessment.

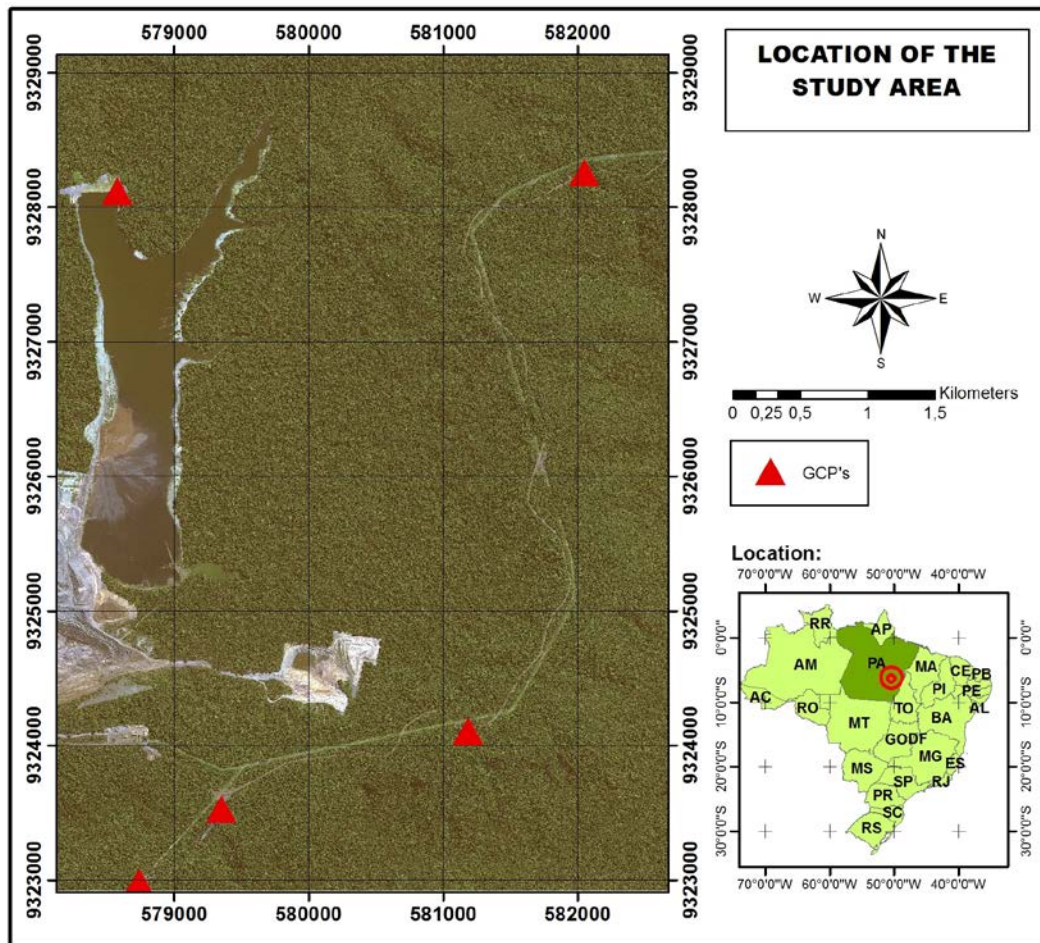


Figure 1. Area of interest and GCPs, in the state of Pará – Brazil.

2. Materials and Method

The GeoEye-1 satellite was developed by GeoEye Incorporation and is able to acquire images of 0.41 m spatial resolution in the panchromatic band (spectral range 450-800 nm) and spatial resolution of 1.65 m in multispectral bands, four at intervals of 450-510 nm (blue), 510-580 nm (green), 655-690 (red) and 780-920 nm (near infrared). The imaging range (swath) corresponds to 15.2 km. The system operates in sun-synchronous orbit at an altitude of 681 km, inclination of 98 degrees, which is able to imaging 350,000 km² per day. GeoEye-1 stereoscopy along-track mode displays great versatility of imaging, with off-nadir angles varying from 0 to 60 degrees.

Stereoscopic image acquisition over Carajás Mining Complex occurred in July 1th, 2012. The first scene has been taken with azimuth and elevation angles of 29.4 and 82.4 degrees, respectively. The second acquisition occurred with azimuth and elevation angles of 39.6 and 51.7 degrees.

The stereoscopy data were processed by Paradella and Cheng (2013) with 0.5 m of spatial resolution (panchromatic and multispectral bands merged). The rational polynomial coefficients - RPCs were retrieved from the metadata. Paradella and Cheng (2013) used an empirical model to generate the DEM, which was based on RPCs. It is a generic sensor model, used as an alternative to rigorous mathematical model and makes full use of satellite images auxiliary parameters.

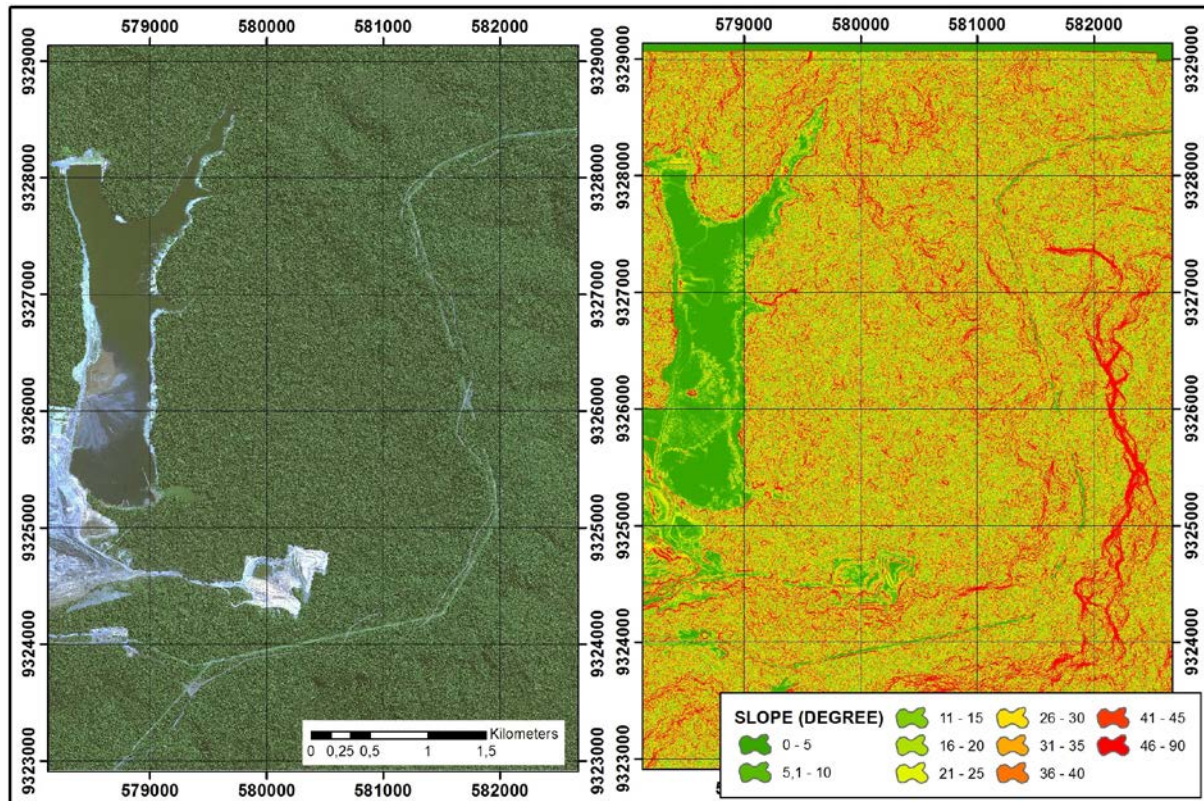


Figure 2. GeoEye-1 natural color composite RGB 321 image (left). DEM generated from stereo pair (right).









Registration was performed with an image to map approach, i.e., attributing UTM coordinates to known features in the image. A number of 5 GCPs were collected by Oliveira (2005) *in situ* through DGPS receivers of two frequencies (L1/L2 - Legacy GGD Javad), in static acquisition mode. Besides auxiliary data, the GCPs contain easting, northing and elevation data. The image was registered to a Universal Transverse Mercator projection, datum WGS-84, zone 22S. The warping method was a polynomial transformation of first order, with nearest neighbor resampling. Image warping, according to Gasbley and Mardia (1998), is a transformation that maps positions in one image plane and attribute these positions in a second plane.

Orthorectification was applied with the same 5 GCPs used in the registration process. This step requires that RCPs are known, once it is important to know information about the sensor ephemerids and attitude errors at the moment of image acquisition (XIONG and ZHANG, 2009). The orthorectification method used was a Toutin's rigorous model, which is based on photogrammetric principles, such as satellite position, sensor attitude, atmospheric refraction, terrain morphology, and cartographic projection transformation (BAIOCCHI et al., 2005).

A supervised classification was applied in both processed images in order to provide a qualitative evaluation of improvement within the registered and orthorectified images. To do

so, it was carried out a supervised classification by the maximum likelihood method, once this method has been well known in scientific literature to display trustful results for high-spatial resolution images (KUPLICH and MARTIN, 2009; Silva et al., 2011; PENHA et al., 2013). Four classes (water, forest, urban, and bare soil) were used in the classification process (Table 1). Ten samples were collected for each class on both images; the samples were geographically identical for the two images.

Table 1. Classification classes, GeoEye-1 natural color composite RGB 321 image and its correspondence in the field (photos taken by Oliveira, 2005).

1	Water		
2	Forest		
3	Urban		
4	Bare Soil		

A nonparametric test was applied in order to validate whether the topographic correction used in this work have improved the geometric quality of the image. To do so, a previously orthorectified image from RapidEye satellite/sensor was used as reference to compute the Root Mean Square Error – RMSE (Equation 1) for both images: georeferenced and orthorectified. The RapidEye images have spatial resolution of 5 m and are orthorectified by the reseller company with the aim of RCPs, GCPs and DEM (COSTA et al., 2015). In spite of

the poorest spatial resolution compared to the GeoEye-1 images, the RapidEye images present a better location accuracy so do are able to be used as reference.

The RMSE was computed for image matching GCPs between the reference and the tested images. It is worth noting that the same GCPs have been used for both images, and they were generated automatically.

$$\text{RMSE} = \sqrt{\frac{1}{n} \sum_{i=1}^n (\varepsilon_{ui}^2 + \varepsilon_{vi}^2)}, \quad (1)$$

where n = number of GCPs, ε_{ui} and ε_{vi} are the GCPs residuals in the u and v coordinates, respectively.

The statistical test used hereby was the Wilcoxon signed-rank test. This is a test used when residuals are non-normally distributed (nonparametric). The test is based on sign and rank magnitude of the difference between paired measurements. The null hypothesis for this test is that the difference of two population distribution are symmetrical about zero, and the alternative hypothesis is that their difference vary, i. e., the difference between the two population distribution is not symmetrical (CARREIRAS et al., 2006). In this work, the null hypothesis is that there is no improvement between a registered and orthorectified image compared to a reference. On the other hand, the alternative hypothesis is that there is improvement between a registered and orthorectified image.

The spatial distribution the GCPs used in the statistical validation are shown in Figure 3.

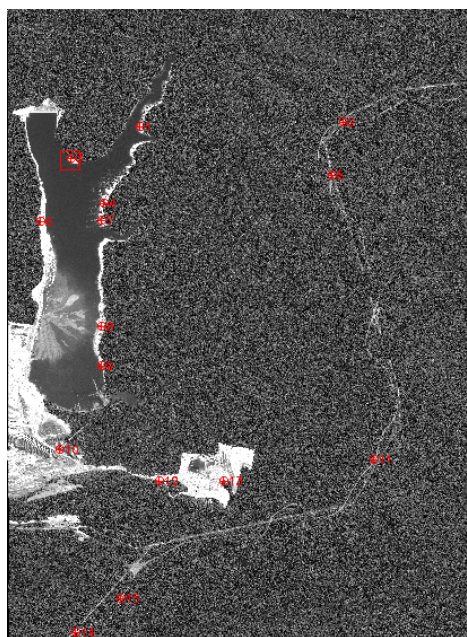


Figure 3. Spatial distribution of validation GCPs.

3. Results and Discussion

In a qualitative approach the difference between the classification of the registered and orthorectified images are shown in Figure 4, for the four classes. Location biases vary from almost zero to 300 m. It is was also noted that the differences are greater in highly steep terrain (Figure 4, bare soil example) and lower in flat terrain as in the lake margin (Figure 4, water example). This is expected once the orthorectification process is a procedure that model

terrain features into a planimetric plane, i. e., the image is considered as a sheet that is overlaid on terrain (DEM).

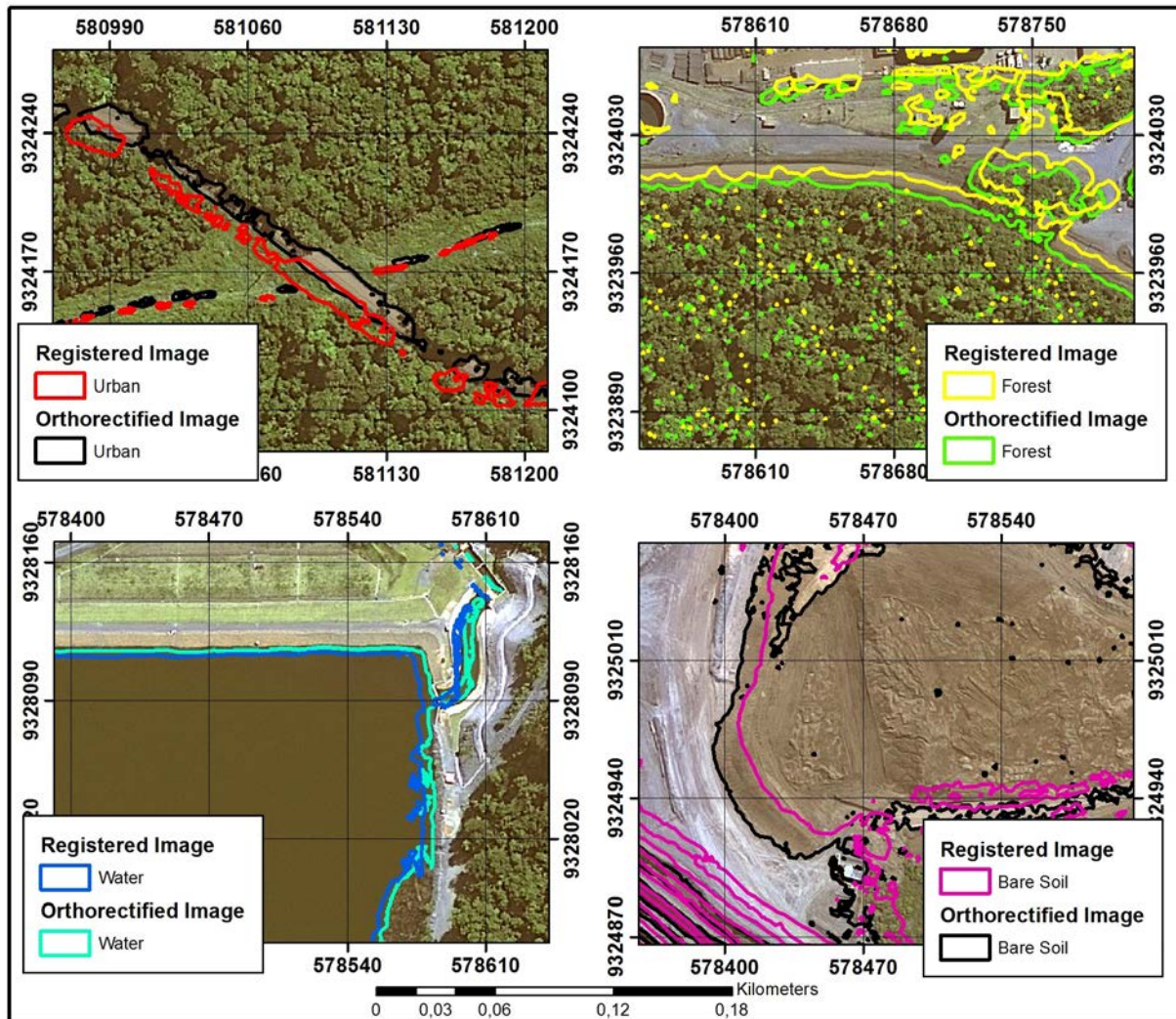


Figure 4. Examples of displacement for each classification class.

From Table 2 it is possible to observe that variations in total area are present. Even though differences are small, they portraint an interest fact. Differences are greater on the forest class, the one with the steepest terrain (Figure 2). On the other hand, the smallest different is observed in the most flat terrain, the water. In addition, for the classes located in steep terrain the area was greater for the registered image, rather the other way.

Table 2. Classes area for each class and for both geometric correction methods.

Classes	Registered (Km ²)	Orthorectified (Km ²)	Difference
Water	1,19	1,22	2,87%
Forest	29,67	27,73	6,56%
Bare soil	31,39	30,87	1,68%
Urban	2,02	2,13	5,00%

Although the classification results have shown that there is a significant difference between the images, results haven't shown whether the orthorecfcation process proved to be

more accurate than the registration compared to a reference. The use of the Wilcoxon signed-rank test proved that in fact the orthorectification process improve the image geometric accuracy at a 5% significance level. This is true, once the statistics $W = 13$ is lower than a critical value related with its significant level, which make us accept that the null hypothesis is not true, i. e., the RMSE of both images are not equal and the direction of improvement is observed in the use of orthorectification.

The RMSE of GCPs are presented in Table 3, it is also shown the difference and the signed-rank for the Wilcoxon test. Based on the validation GCPs (collected randomly), the mean RMSE for the registered image is 13.0 and 7.6 for the orthorectified image, showing an improvement of almost two fold in accuracy between the two processes.

Table 3. Validation GCPs for the orthorectified and registered image, as well as the data to perform the Wilcoxon test.

GCPs	Orthorectificac RMSE	Registered RMSE	Difference	Signed- rank
1	5,55	2,59	-2,96	-4
2	1,31	22,67	21,36	11
3	10,24	9,55	-0,69	-2
4	8,18	7,59	-0,59	-1
5	5,97	7,39	1,42	3
6	2,25	14,68	12,43	9
7	20,01	27,03	7,02	7
8	6,81	17,23	10,42	8
9	6,49	10,33	3,84	5
10	8,04	23,21	15,17	10
11	6,71	0,71	-6,00	-6

4. Conclusions

In this work we presented an evaluation of registration and orthorectification geometric correction methods. In order to do that a supervised classification was applied, as well as a statistical evaluation of the RMSE. Results have shown that location shifts are present between the registered and orthorectified image. There are also differences in the total area of each class, mostly on steep terrain. The statistical analysis has proved that there is improvement in the use of the orthorectification process at a 5% significance level.

As aforementioned, we could conclude that the orthorectification process is an important step on image geometric correction, contributing to enhance image metrics, morphology, and even so location accuracy.

This work consolidate an old established concept: that terrain plays a major role on remotely sensed image geometry. This highlights the importance of using DEMs to correct high-spatial resolution images from geometric biases caused by terrain morphology. A technique that feed both means is the use of stereo capable sensors as they can produce a DEM at the same moment of image acquisition.

5. References

Baioacchi, V.; Crespi, M.; De Vendictis, L.; Giannone, F. A new rigorous model for the orthorectification of synchronous and asynchronous high resolution imagery. In: *New Strategies for European Remote Sensing*, 2005. **Proceedings...** Rotterdam: Millpress, 2005.

Carreiras, J. M. B.; Pereira, J. M. C.; Pereira, J. S. Estimation of tree canopy cover in evergreen oak woodlands using remote sensing. **Forest Ecology and Management**, v. 223, p. 45-53, 2006.

Cerqueira, J. D. M. **Ortorretificação Digital de Imagens de Satélites de Alta Resolução Espacial**. Recife: UFPE, 2004.

Costa, C. R.; Luz, N. B.; Araki, H.; Oliveira, Y. M. M.; Rosot, M. A. D.; Garrastazú, M. C.; Krueger, C. P. Análise da exatidão cartográfica das imagens RapidEye adotadas no Inventário Florestal Nacional do Brasil (IFN-BR). In: Simpósio Brasileiro de Sensoriamento Remoto (SBSR), 17., 2015, João Pessoa. **Proceedings...** São José dos Campos: INPE, 2015. p. 3289-3296. Available at: <<http://www.dsr.inpe.br/sbsr2015/files/p0651.pdf>>. Accessed in: aug.31.2015.

Freitas, G. M.; Esquerdo, J. C. D. M.; Korbes, A. Registro de imagens NOAA através de correlação de fase. In: Simpósio Brasileiro de Sensoriamento Remoto (SBSR), 13., 2008, Campinas. **Proceedings...** São José dos Campos: INPE, 2008. Papers, p. 6883-6887.

Flusser, J.; Suk, T. A moment-based approach to registration of images with affine geometric distortion. **IEEE Transactions on Geoscience and Remote Sensing**, v. 32, p. 382-387, mar. 1994.

Gasbley, C. A.; Mardia, K. V. A review of image warping methods. **Journal of Applied Statistics**, v. 25, p. 155-177, 1998.

GeoEye Satellite Sensor specifications. Available at: <<http://www.satimagingcorp.com/satellite-sensors/geoeye-1/>>. Accessed in: aug.28.2015.

Kuplich, T. M.; Martin, E. V. Identificação de tipologias da vegetação campestre e o uso de imagem Thematic Mapper (Landsat 5) na região dos Campos de Cima da Serra, Bioma Mata Atlântica. In: Simpósio Brasileiro de Sensoriamento Remoto (SBSR), 14., 2009, Natal. **Proceedings...** São José dos Campos: INPE, 2009. p. 2769-2775. Available at: <<http://urlib.net/dpi.inpe.br/sbsr@80/2008/11.18.00.43>>. Accessed in: aug.31.2015.

Mao, Z. et al. Automatic registration of seawifs and avhrr imagery. **International Journal of Remote Sensing**, v. 22, p. 1725-1735(11), 2001.

Oliveira, K. G. **Avaliação de Modelos Digitais de Elevação Gerados a partir de Sensores Remotos Orbitais Óptico (Aster) e Radar (RADARSAT-a, SRTM): um Estudo para Região da Serra dos Carajás**. 2005. 184 p. (INPE-13168-TDI/1027). Dissertation (Master in Remote Sensing) – Instituto Nacional de Pesquisas Espaciais, São José dos Campos. 2005.

Paradella, W. R.; Cheng, P. Using GeoEye Stereo Data in Mining Application Automatic DEM Generation. **GeoInformatics**, p. 10-12, 2013.

Penha, T. V.; Silva, J. M. M.; Prado, R. B.; Fidalgo, E. C. C. Ortorretificação e classificação de imagens dos satélites de alta resolução World View2 e GeoEye. In: Simpósio Brasileiro de Sensoriamento Remoto (SBSR), 16., 2013, Foz do Iguaçu. **Proceedings...** São José dos Campos: INPE, 2013. p. 1379-1386. Available at: <<http://urlib.net/3ERPFQTRW34M/3E7GC69>>. Accessed in: aug.31.2015.

Silva, A. R.; Tomasiello, D. B.; Prado, B. R.; Vieira, M. A.; Barbarisi, B. F.; Ortiz, M. J. Extração da cobertura vegetal de áreas urbanas utilizando imagens do satélite GeoEye-1. In: Simpósio Brasileiro de Sensoriamento Remoto (SBSR), 15., 2011, Curitiba. **Proceedings...** São José dos Campos: INPE, 2011. p. 1576-1583. Available at: <<http://urlib.net/3ERPFQTRW/3A2L2NP>>. Accessed in: aug.31.2015.

Schowengerdt, R. A. **Remote Sensing: Models and Methods for Image Processing**. Third Edition. University of Arizona, 2007. p. 363-365.

Xiong, Z.; Zhang, Y. A Generic Method for RPC Refinement Using Ground Control Information. **Photogrammetric Engineering and Remote Sensing**, v. 75, n. 9, p. 1083-1092, 2009.